BUTTERWORTH HEINEMANN

Polymer Vol. 36 No. 16, pp. 3059–3069, 1995

0032-3861/95/$10.00+0.00

polymer papers

Differential scanning calorimetry and optical microscopy investigations of the isothermal crystallization of a poly(ethylene oxide)–poly(methyl methacrylate) block copolymer

P. H. Richardson and R. W. Richards*
Interdisciplinary Research Centre in Polymer Science and Technology, University of Durham, South Road, Durham DH1 3LE, UK

and D. J. Blundell, W. A. MacDonald and P. Mills
ICI plc, Wilton Materials Centre, Wilton, Middlesbrough, Cleveland, Teesside TS6 8JE, UK
(Received 28 March 1994; revised 9 February 1995)

The isothermal crystallization of the poly(ethylene oxide) block in a linear diblock copolymer of poly(methyl methacrylate)–poly(ethylene oxide) with a poly(ethylene oxide) weight fraction of 0.76, has been evaluated using optical microscopy and differential scanning calorimetry. The copolymer was quenched from the melt to a range of crystallization temperatures between 289 K and 316 K and the crystallization monitored by observation of the increase in radius of spherulites (microscopy) or the enthalpy of fusion (calorimetry) as a function of time. Comparison experiments were also made on physical blends of the two homopolymers where the weight fraction of polyethylene oxide ranged from ~0.6 to 0.9. The block copolymer has an observed melting point which is 2–3 K lower and the spherulite growth rate was reduced compared with the equivalent blend. The growth rates calculated from optical microscopy have been subjected to crystallization regime analysis. All three regimes are observable in the block copolymer for the supercooling conditions used here, only regimes I and II are evident for the pure poly(ethylene oxide), and for the blends regime I appears to be completely suppressed. From the regime analysis a fold surface free energy in the block copolymer of 16–20 erg cm^{-2} has been obtained, which is much less than that obtained for the pure poly(ethylene oxide) or the blends. An explanation based on the favourable enthalpy of mixing with poly(methyl methacrylate) is suggested. Enthalpy of fusion data from isothermal crystallization studies on all polymers in the d.s.c. have been analysed using Avrami theory. The Avrami exponent was obtained together with an effective rate constant of crystallization. The exponent suggests that crystallization takes place via homogeneous nucleation with a spherical growth morphology, growth being controlled by the rate of attachment of molecules to the interface. By comparison of the Avrami exponent with values obtained for blends differing only in the molecular weight, the influence of melt viscosity on growth control is evident.

(Keywords: isothermal crystallization; PEO–PMMA block copolymer; Avrami exponent)

INTRODUCTION

An understanding of polymer crystallization kinetics is of importance in the study of many aspects of semicrystalline polymers, e.g. the control of spherulitic size and the determination of fold surface free energy. The conditions under which a polymer crystallizes control both nucleation and spherulitic growth rate; these in turn determine the final spherulite size and the degree of crystallinity. Both the spherulite size and the degree of crystallinity influence the optical and mechanical properties of a polymer. Moreover, the temperature dependence of polymer crystal growth from dilute solution or quiescent melt has an important place in the determination of the mechanisms of polymer crystallization. The Avrami analysis of crystallization kinetics was adapted from theories[1,2] originally developed for metals. Although the Avrami parameters obtained provide insight into macroscopic controlling factors, they do not provide a *molecular* description of polymer crystal growth. A much more molecularly based analysis and one which connects to the reptation theory of polymer melt diffusion is the kinetic nucleation theory expounded by Hoffman *et al.*[3–5] which defines three regions (regimes) of crystal growth. Experimental evaluation of this theory has been extensively discussed using data for polyethylene; however, other polymers have also been investigated from this viewpoint. Of particular relevance here are the detailed studies of poly(ethylene oxide) reported by Kovacs *et al.*[6–10], Ding and Amis[11] and Cheng *et al.*[12–14].

Extensive studies have also been carried out on

* To whom correspondence should be addressed

crystallization in binary mixtures of crystalline and amorphous polymers[15–17]. When two polymers are compatible in the melt (as with poly(ethylene oxide)/poly(methyl methacrylate) (PEO/PMMA) blends[18–23]), the non-crystalline polymer may have a profound influence on the nucleation, crystallization kinetics and final morphology of the crystalline species. Generally, the crystallization in such blends has been investigated using optical microscopy (OM) and differential scanning calorimetry (d.s.c.), since this combination is able to provide both kinetic and thermodynamic parameters for the polymer system. Earlier studies of the isothermal crystallization of PEO/PMMA blends using d.s.c. and OM[15,24–28] have noted several correlations with molecular weight, polydispersity and tacticity. In particular, a negative value for the Flory–Huggins interaction parameter, χ, was observed for temperatures close to and above the melting point of PEO (approximately 338 K), indicating that the two homopolymers are compatible.

Since blending with an amorphous polymer has an influence on the crystallization of semicrystalline polymers, it is anticipated that a block copolymer of the same two components should produce even more significant effects because gross phase separation of the two polymers is prevented. We report here observations on the isothermal crystallization of one PEO-*b*-PMMA block copolymer (76 wt% PEO) using d.s.c. and OM, and Avrami analysis and kinetic nucleation theory in the analysis of the data. To provide a direct comparison with the PEO-*b*-PMMA block copolymer, limited data for blends of the two homopolymers and pure PEO are also presented. These data are part of a larger study on other block copolymers where the PEO content is larger. The crystallization of these latter copolymers is radically different from that of PEO or the single block copolymer discussed here.

THEORETICAL BACKGROUND

Macroscopic crystallization kinetics (Avrami theory)

Johnson and Mehl[1] and Avrami[2] considered the growth of perfectly crystalline material into the supercooled melt; this theory has been adapted for the crystallization of polymers where the crystalline regions contain amorphous polymer. The resultant equation is:

$$X(t) = 1 - \exp(-K_n t^n) \quad (1)$$

where $X(t)$ is the mass fraction of polymer converted in time t and K_n is an effective rate constant for the crystallization process. The exponent n depends on the morphology of the growing crystalline regions, the nucleation process and whether growth is controlled by diffusion of polymer through the melt or attachment to the growth surface. Unfortunately, identical values of n may be obtained by a variety of different growth mechanisms and morphology. Shultz[29] has provided a table of values of n and the conditions under which they are observed. The Avrami parameters (usually confined to n) are obtainable via double logarithmic plots of the time dependence of some property which responds to the volume or mass of crystalline species present.

Kinetic nucleation theory[3–5]

Three regions of crystal growth are predicted by this theory, the kinetics of each being controlled by the competition between nucleation and growth. In regime I, a single nucleation takes place on the substrate surface and leads to the substrate length being completely covered by a crystallization growth layer. At lower temperatures (larger supercooling, ΔT), regime II growth prevails where multiple nucleation takes place on the substrate. At still larger values of ΔT, regime III is entered where nucleation on the substrate is so prolific that the distance between niches approximates to a stem width. For each of these regimes, the crystal growth rate is expressed by:

$$G(i) = \frac{Z}{n^\nu} \Delta T \exp\left(\frac{-U^*}{R(T_c - T_\infty)}\right) \exp\left(\frac{-K_g(i)}{T_c \Delta T f}\right) \quad (2)$$

where i = I, II or III, $\Delta T = T_m^0 - T_c$ with T_m^0 the equilibrium melting temperature, T_∞ is $(T_g - 30)$ K, U^* is the activation energy of reeling in the polymer molecule from its melt reptation tube and f is a temperature correction factor of $2T_c/(T_m^0 + T_c)$. Each regime has a nucleation constant $K_g(i)$, and $K_g(\mathrm{I}) = 2K_g(\mathrm{II}) = K_g(\mathrm{III})$ with:

$$K_g(\mathrm{I}) = 4b\sigma\sigma_e T_m^0/(k_B \Delta h_f) \quad (3)$$

with b the stem width, σ and σ_e the lateral and fold surface free energies respectively, k_B Boltzmann's constant and Δh_f the enthalpy of fusion per monomer unit per unit volume. The Z parameter contains mobility terms, n is the degree of polymerization and ν is related to a parameter λ, the value of which is determined by the sweep angle of the molecule after its first attachment to the substrate. In regime I, $\nu = 1 + \lambda$ and in regime II, $\nu = 1 + \lambda/2$.

EXPERIMENTAL

Synthesis of PEO-b-PMMA block copolymer

The block copolymer, BC76, was synthesized by anionic polymerization under high vacuum using diphenyl methyl potassium as initiator. A known quantity of methyl methacrylate (MMA) dissolved in THF (approx. 5% w/w) was anionically initiated at 197 K using an appropriate quantity of initiator according to the molecular weight desired. A small amount of the 'living' PMMA solution was collected in a side-arm for future isolation and analysis. After 2–3 h, a known quantity of ethylene oxide (EO) was added to the 'living' PMMA solution which was then allowed to warm slowly to room temperature overnight. At this point the flask and contents were heated at 348 K for 4 days. The 'living' block copolymer was terminated by injection of a small quantity of degassed acetic acid and isolated by precipitation in hexane and dried under vacuum at 313 K. The block copolymer was characterized by size-exclusion chromatography and ^{1}H and ^{13}C n.m.r.; the results of the characterization are reported in Table 1.

Polymer blends

The homopolymers, poly(ethylene oxide) (PEO), M_p = 18 600, polydispersity = 1.06, and poly(methyl methacrylate) (PMMA), M_p = 22 200, polydispersity = 1.07, were supplied by Polymer Laboratories (Church

Stretton, UK) and a series of blends varying in composition were prepared by dissolving known quantities of each homopolymer in chloroform (5% w/w), followed by precipitation in hexane. The blends were dried in a vacuum oven at 313 K for 3 days, and stored in a desiccator in the dark. Four blend mixtures were prepared, BL90, BL80, BL70 and BL60, the numbers being indicative of the weight fraction of PEO in each blend.

Optical microscopy

Thin films (~4 μm thick) of BC76, the blends and PEO were cast onto glass cover slips at room temperature from 5% w/w chloroform solutions. After allowing the solvent to evaporate slowly in air, the films were annealed at 313 K under vacuum for 48 h to remove all traces of solvent. After annealing, the cover slip was placed on a Linkam hot stage mounted on an Olympus optical microscope. The polymer film was covered by a second cover slip, and rapidly heated to 423 K where it was held for 10 min to remove any thermal history. The sample was then quenched at the controlled rate of 100 K min^{-1} to selected crystallization temperatures, T_c. The subsequent growth of crystalline species after quenching was viewed between crossed polars and recorded by a video camera. The growth rate G ($= dR/dt$, with R the spherulite radius) was determined by measuring the radius of the spherulite as a function of time during the isothermal crystallization process. The spherulitic radius was measured directly from the video-recorded image. To obtain the growth rate, the $t = 0$ value was obtained by extrapolating the observed spherulite radius, R_t, to zero and noting the time for which $R_t = 0$. The observed times were then 'corrected' by subtracting this 'zero time' from the experimental times. After leaving the sample for 120 min at each T_c, the apparent melting point temperature, T_m' was recorded using the hot-stage microscope and a heating rate of 10 K min^{-1}. The temperature, T_m', was the point at which the birefringence associated with the presence of crystalline species was no longer visible, the influence of heating rate on T_m' was negligible. Values of T_c ranged from 289 K to 315 K for the block copolymer and 289 K to 323 K for the blends and PEO. For each crystallization temperature, at least five separate growth rates were determined and the average calculated.

Table 1 Characteristics of the PEO-*b*-PMMA block copolymer BC76

PEO/PMMA (% w/w)	Total M_w[a]	Polydispersity of PEO-*b*-PMMA	M_W of PMMA[b]	Polydispersity of PMMA
76/24	82900	1.60	19700	1.05

Tacticity ratios: 5.5 : 4.0 : 1 (atactic : syndiotactic : isotactic)
[a] $CHCl_3$ solvent s.e.c.
[b] THF solvent s.e.c.

Differential scanning calorimetry: isothermal crystallization

The isothermal crystallization kinetics of BC76, the series of blends and PEO were determined by monitoring

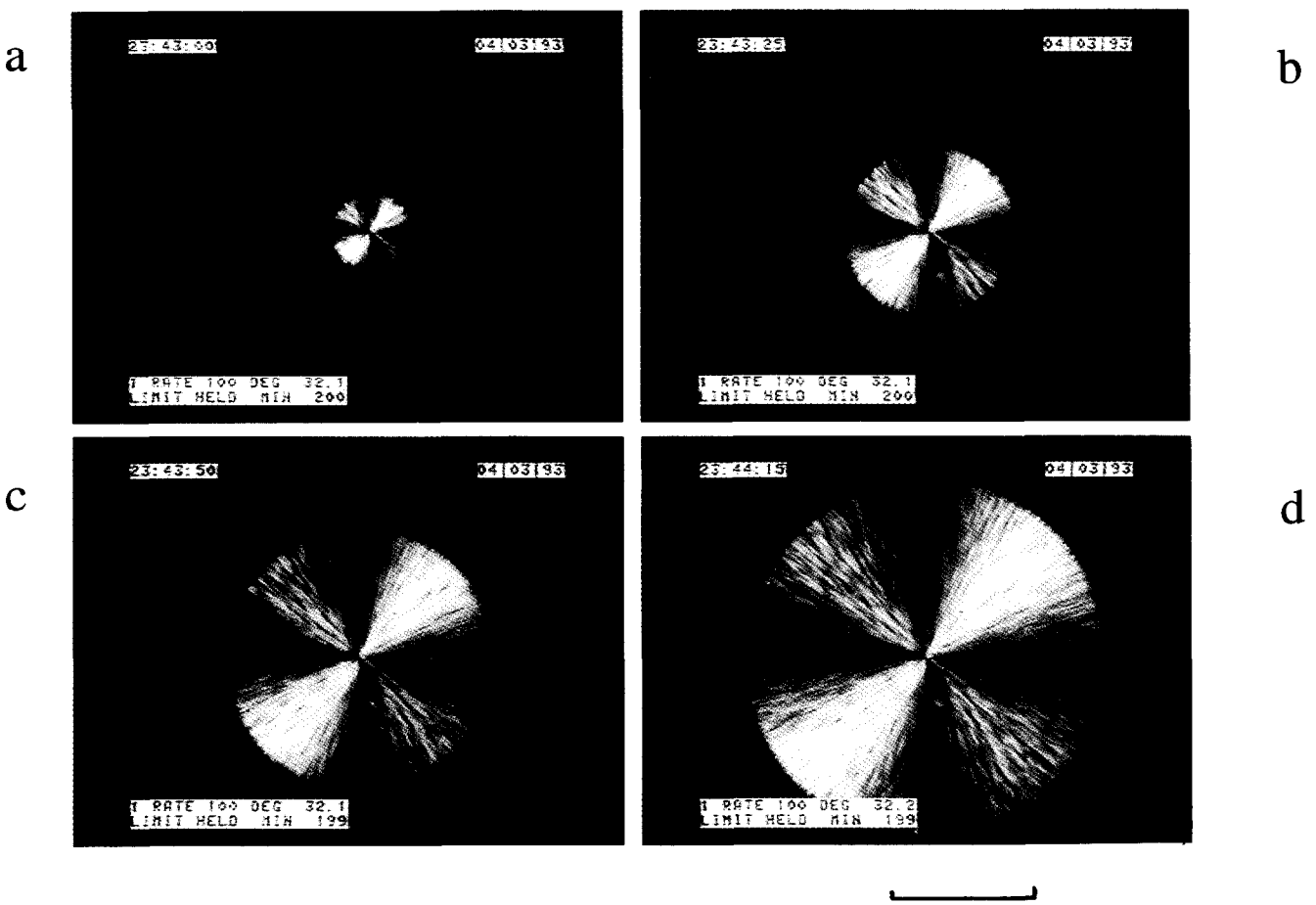

Figure 1 Isothermal spherulite growth for BC76 at various times, t, after quenching to 305 K: (a) 20 s; (b) 45 s; (c) 70 s; (d) 95 s. Scale marker = 100 μm

the crystallization exotherm as a function of time for various values of T_c. A Perkin–Elmer DSC 7 calorimeter, calibrated using indium and zinc, was used to monitor isothermal crystallization. Approximately 10 mg of sample was annealed at 423 K for 10 min to remove any thermal history, and then quenched to specific T_c values at the controlled cooling rate of 100 K min^{-1}. The crystallization exotherm was then recorded as a function of time.

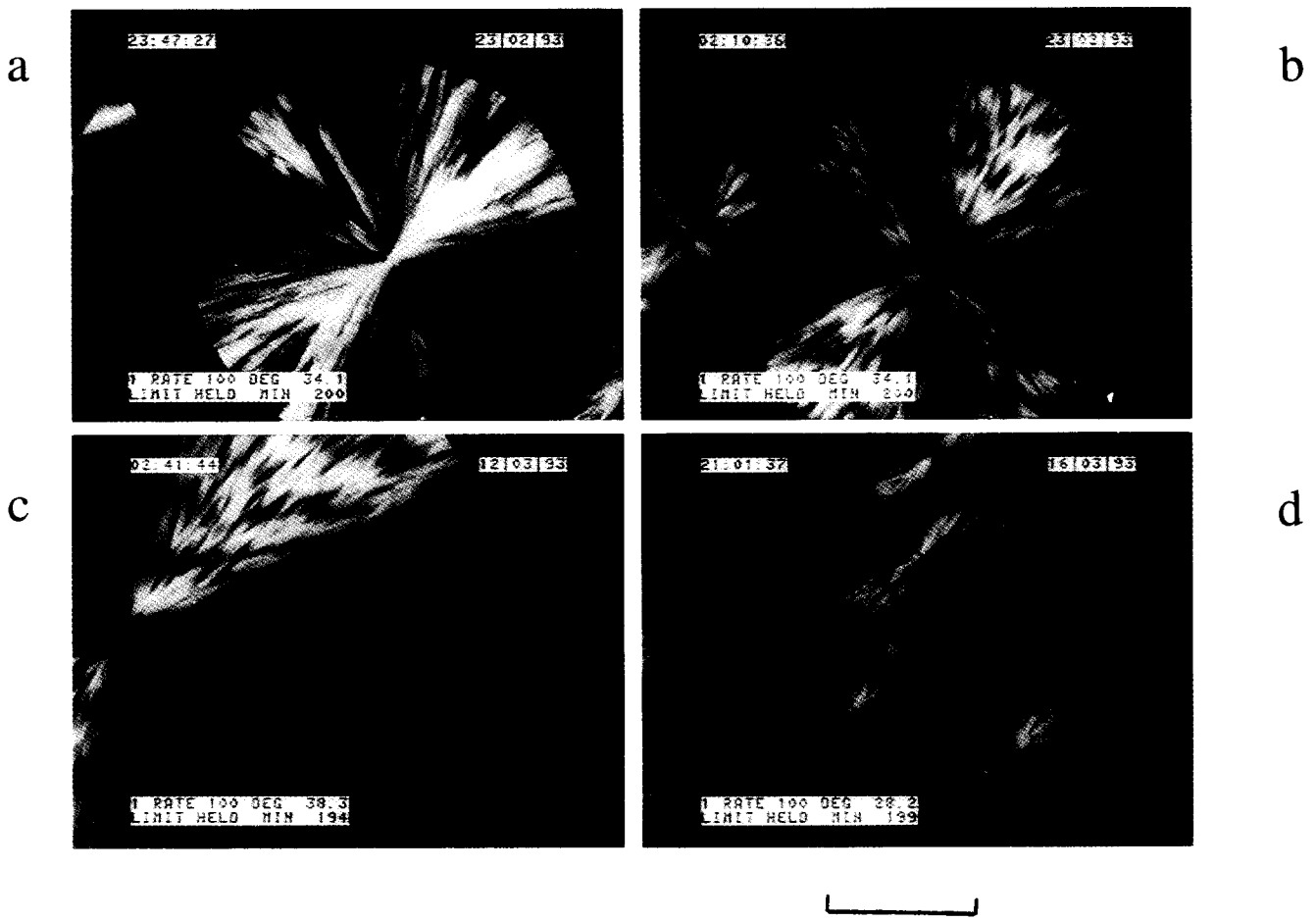

Figure 2 Variation in spherulitic texture as a function of PMMA content in PEO/PMMA blends. (a) BL90 at T_c = 307 K; (b) BL80 at T_c = 307 K; (c) BL70 at T_c = 311 K; (d) BL60 at T_c = 301 K. Scale marker = 100 μm

Table 2 Crystallization temperatures, T_c, and observed melting temperatures, T_m, for BC76 using optical microscopy

T_c (K)	315	313	311	309	307	305	303	301	299	297	295	293	291	289
T_m'	328.9	328.5	328.1	327.1	326.9	326.8	326.8	326.8	326.9	327.0	327.0	327.0	327.0	327.0

Table 3 Crystallization temperatures, T_c, and observed melting temperatures, T_m, for PEO and blends using optical microscopy

PEO													
T_c	323	321	319	317	315	313	311	309					
T_m'	333.8	333.7	332.1	331.6	331.2	331	331.0	330.9					
PEO/PMMA (90/10) BL90													
T_c	315	313	311	309	307	305	303	301					
T_m'	328.9	329.9	328.4	328.6	328.6	328.2	328.7	328.3					
PEO/PMMA (80/20) BL80													
T_c	317	315	313	311	309	307	305	303	301				
T_m'	330.5	330.1	330.4	330.2	328.8	328.5	328.4	327.9	327.6				
PEO/PMMA (70/30) BL70													
T_c	313	311	309	307	305	303	301	299	297	295	293	291	289
T_m'	329.9	329.9	329.7	329.7	329.4	329.3	329.5	329.3	328.5	328.9	328.6	328.5	328.5
PEO/PMMA (60/40) BL60													
T_c	313	311	309	307	305	303	301	299	297	295	293	291	289
T_m'	327.5	327.3	326.6	326.8	326.9	326.7	326.5	327.0	327.3	327.7	327.8	329.3	329.9

All values in degrees Kelvin

RESULTS

Optical microscopy

Figure 1 shows a typical micrograph for the isothermal crystallization of BC76 at 305 K. The positive Maltese cross extinction pattern is evident (i.e. bright regions at 45° to the meridian), indicating perpendicular or parallel orientation of the crystalline molecular axis with respect to the spherulitic radius[30,31]. There was no marked difference between the spherulitic textures of the blends and the block copolymer. A reduction in the number of nucleation sites and consequently a reduction in the number of spherulites formed was observed as T_c increased. The observed maximum spherulitic radius increased, ranging from 100 to 1000 μm (T_c = 289–315 K), as T_c increased. As the amount of PMMA in the blends increased, the morphological texture became more open and less ordered (*Figure 2*). For BC76, the blends and PEO, the apparent melting point, T_m', decreased with T_c; additionally, for the blends, a decrease in T_m' was observed as the amount of PMMA increased (*Tables 2* and *3*). A reduction of 2–3 K in T_m' was observed for BC76 with respect to the corresponding blend.

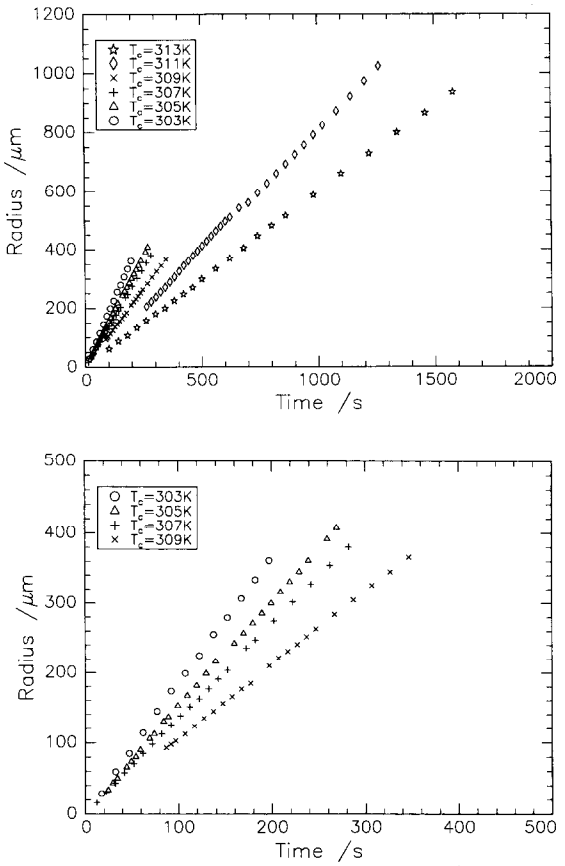

Figure 3 Spherulite radius as a function of time at the crystallization temperatures, T_c, indicated for the block copolymer BC76

Figure 3 shows a plot of the spherulitic radius, R, against time, t, at each crystallization temperature for BC76. For all temperatures, the spherulitic radius increased linearly with time. It was observed that for high values of T_c, and at very long times of isothermal crystallization, the growth rate decreased. Furthermore, the induction time for nucleation became more protracted for these higher values of T_c. For a given T_c, all of the spherulites were not nucleated instantaneously (i.e. sporadic nucleation prevailed); however, once nucleated each spherulite grew at the same growth rate, G. The spherulitic growth rate was determined from the gradient of the spherulitic radius *versus* time plot.

Differential scanning calorimetry: isothermal crystallization

Figure 4 shows d.s.c. thermograms obtained for the isothermal crystallization of BC76 at various crystallization temperatures and *Figure 5* compares the isothermograms for BL80 and BC76 at T_c = 313 K. It is

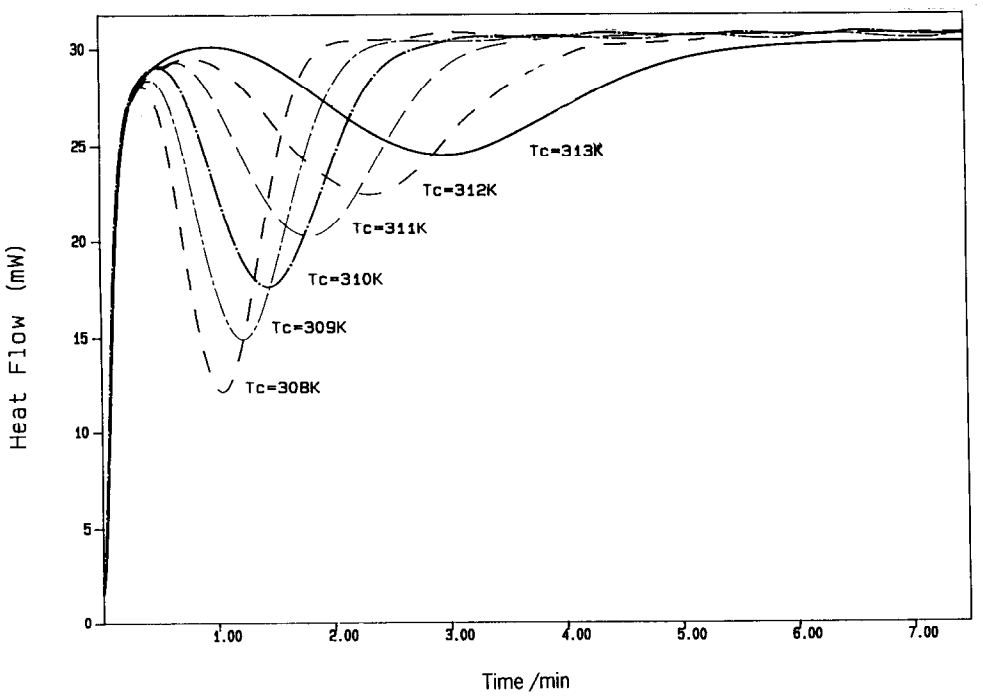

Figure 4 Isothermograms obtained from d.s.c. for BC76 at the values of T_c indicated on each curve

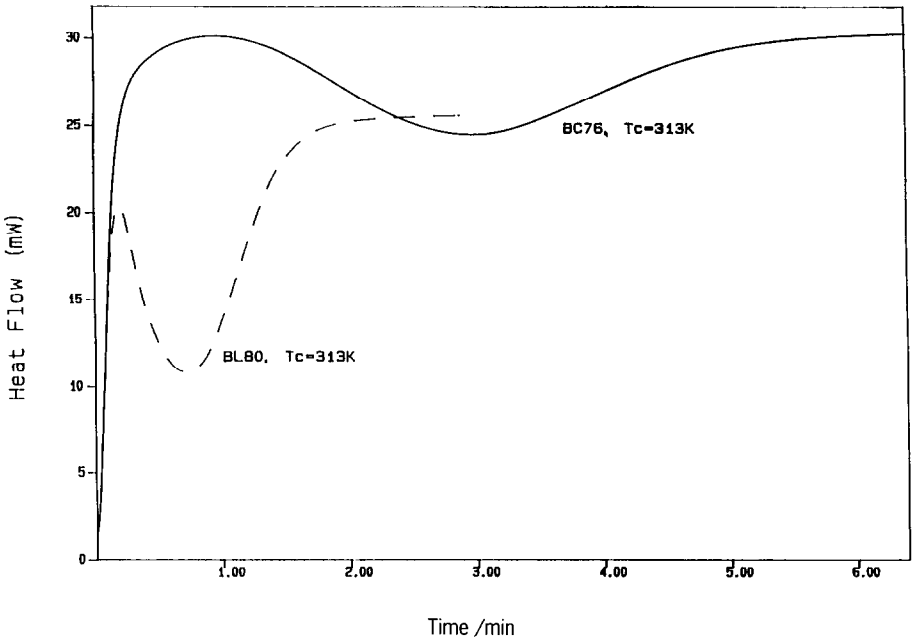

Figure 5 Isothermograms at $T_c = 313$ K for BC76 and the PEO/PMMA blend BL80

Table 4 Equilibrium melting points for PEO, BC76 and blends

Sample	Equilibrium melting point, T_m (K)
PEO	336.5
PEO/PMMA (90/10) BL90	332.6
PEO/PMMA (80/20) BL80	333.4
PEO/PMMA (70/30) BL70	331.4
PEO/PMMA (60/40) BL60	328.5
PEO-*b*-PMMA (76/24) BC76	330.8

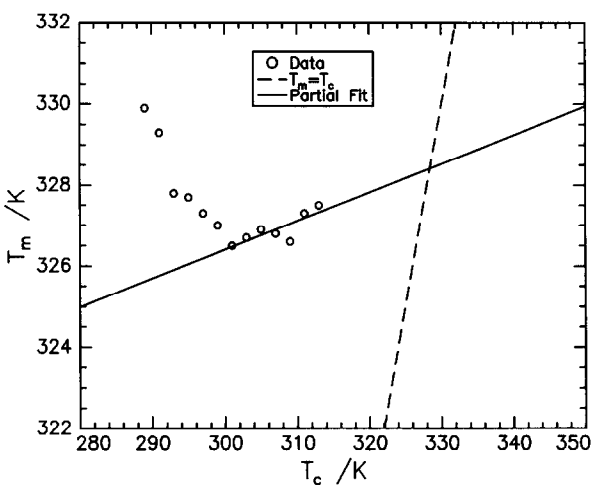

Figure 6 Hoffman–Weeks plot for BL60 illustrating the increase in T_m' at low values of T_c. Solid line is a linear least-squares fit to the data for $300\,K \leq T_c \leq 315\,K$

evident that the rate of crystallization of the block copolymer is appreciably slower than that of the blend.

DISCUSSION

Optical microscopy: equilibrium melting points and melting point depression

The isothermal crystallization behaviour of the blends was similar to that previously reported[15,25–28,32]. The observed linear growth with time implies that the concentration of PMMA at the tips of the radial lamellae does not change. It has been suggested that the rejected, non-crystallizable PMMA becomes trapped between the growing fibrils of the spherulite. This suggestion is supported by the observation of less regular, more feather-like morphology as the amount of PMMA in the blend increases, *Figure 2*, and from small-angle X-ray scattering data where the observed amorphous interlamellar spacing increased with PMMA concentration[33]. For high T_c values and at very long isothermal crystallization times, this linear growth rate decreases. It has been suggested that this is due to the growth becoming more dependent on the amount of locally available PEO and consequently, dependent upon the diffusion of the crystallizable PEO fraction[34] to the crystallization site. Crystal growth is now under a concentration gradient formed near the growth front due to segregation of the diluent and can be interpreted in terms of the Cahn theory[35]. However, the influence of crystallization regime must not be ignored (see below).

The melting temperatures, T_m', have been used in Hoffmann–Weeks[36] plots to obtain the equilibrium melting temperature, T_m^0, for each system and these are reported in *Table 4*. For BL60, unusual melting behaviour was observed at large values of supercooling. At a particular value of T_c ($\sim$298 K), an increase in T_m' was observed and the melting point continued to increase as T_c decreased further (i.e. ΔT increased). Consequently, the extrapolation to obtain T_m^0 in the Hoffmann–Weeks plot could only be done on a subset of the data (*Figure 6*). Martuscelli and Demma[32] have observed non-linear depression of the melting point in PMMA/PEO blends for large values of ΔT which they attribute to phase separation and lower critical solution temperature behaviour. However, results from separate small-angle neutron scattering experiments[37] show that the polymer–polymer interaction parameter for PMMA/PEO blends has a positive temperature coefficient and thus high temperatures are favourable to mixing. The

observed increase in T_m' is therefore due to an upper critical phase boundary being crossed. As the boundary is crossed the blend demixes into two phases, with one phase having a higher PEO content than the blend average, and thus a higher melting temperature is observed. The second phase has such a low content of PEO that no crystallization is observed.

We have used the Nishi–Wang[38] expression to obtain the polymer–polymer interaction parameter to check that the thermodynamics of these blends is no different from that in earlier discussions of such blends. The Nishi–Wang expression is:

$$(T_{mc}^0 - T_m^0) = -T_{mc}^0[V_2/\Delta_{fus}H]B\phi_1^2 \qquad (4)$$

with

$$B = RT\chi/V_1$$

where T_m^0 is the equilibrium melting point of the blend and T_{mc}^0 is the equilibrium melting point of the pure semicrystalline polymer in the blend, V_1 and V_2 are the molar volume of the amorphous and semicrystalline polymer respectively and ϕ_i is the volume fraction of component i. Values used for V_1 and V_2 were $85.6\,cm^3\,mol^{-1}$ and $38.9\,cm^3\,mol^{-1}$ respectively and the enthalpy of fusion of PEO ($\Delta_{fus}H$) has the value of $8.79\,kJ\,mol^{-1}$, χ is the interaction parameter between the two polymers. *Figure 7* shows the melting point data plotted according to equation (4). From the slope of this plot, the value of B obtained is $-19.2\,J\,cm^{-3}$ which results in $\chi = -0.52$ at the equilibrium melting temperature of 336.5 K. This value is in agreement with values reported elsewhere for PEO/PMMA blends with different molecular weights[18,32,39] and signifies that there is no significant influence of molecular weight on the bulk thermodynamic parameters of the system which may influence the crystallization kinetics. We do not place any significance on the intercept of *Figure 7*; only a limited number of blend compositions have been studied here and consequently this intercept may be an artefact.

Crystallization growth rate and regime analysis

We now attempt a crystallization regime analysis of the data for the blends and the block copolymer to ascertain the influence of copolymer structure *vis à vis* blend organization on the crystallization process. No distinct difference in the crystalline morphologies of the block copolymer and the corresponding blend was noted. However, the rate of crystallization of the block copolymer was considerably reduced (3–4-fold decrease in G at a specific T_c for BC76 with respect to BL80, *Figure 8*) and the melting point is reduced (approximately 2–3 K). Donth *et al.*[40] have demonstrated that mobile free ends are required during the crystallization, the observed reduction may be due to an effective halving of the crystallizable mobile ends in the block copolymer relative to the equivalent blend. The spherulitic growth rates determined here are larger than those reported by Martuscelli *et al.*[33] for PEO/PMMA blends of higher molecular weight. However, it should be noted that the crystallization temperatures used by us were appreciably lower than those in previous studies[15,25–28,32].

Figure 8 shows semilogarithmic plots of the crystallization growth rate as a function of the supercooling, ΔT, for all systems except BL60 which has the anomalous melting behaviour remarked on earlier. For

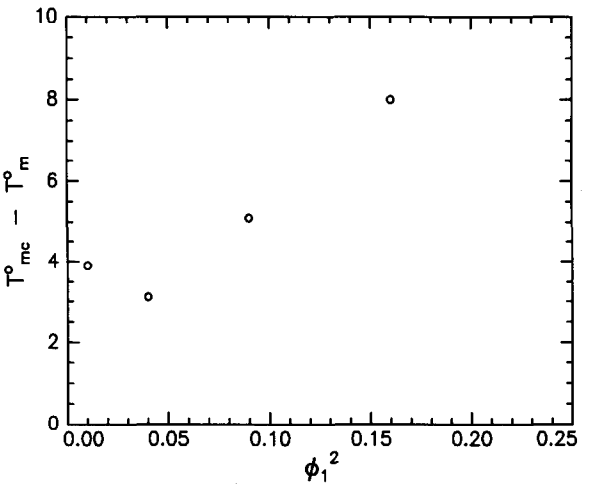

Figure 7 Melting point depression ($T_{mc}^o - T_m^o$) for blends of PEO and PMMA plotted according to the Nishi–Wang expression, equation (4), with ϕ_1 the volume fraction of PMMA in the blend

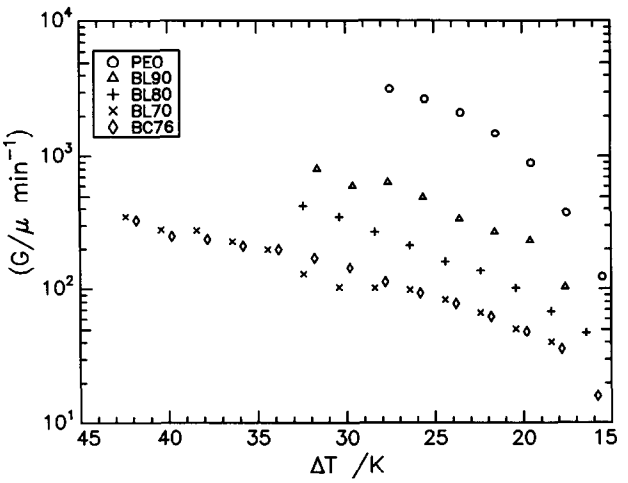

Figure 8 Semilogarithmic plot of growth rate, G, as a function of supercooling, ΔT, for all specimens investigated

some data sets at least two regimes of crystallization behaviour are evident from this figure. Taking natural logarithms of both sides of equation (2), we obtain:

$$\ln G(i) = \ln\left(\frac{Z}{n^\nu}\right) + \ln\Delta T - \frac{U^*}{R(T_c - T_\infty)} - \frac{K_g(i)}{T_c\Delta Tf} \qquad (5a)$$

$$\ln G(i) - \ln\Delta T + \frac{U^*}{R(T_c - T_\infty)} = \ln\left(\frac{Z}{n^\nu}\right) - \frac{K_g(i)}{T_c\Delta Tf} \qquad (5b)$$

Hence a plot of the left-hand side of equation (5b) as a function of $(T_c\Delta Tf)^{-1}$ should be a straight line of intercept $\ln(Z/n^\nu)$ and slope $-K_g(i)$. Since the magnitude of $K_g(i)$ depends on the crystallization regime, a series of straight lines of different slope and intercept should be obtained if more than one growth regime is explored. Evaluation of the left-hand side of equation (5b) requires values of T_g and U^* for PEO, the crystallizable component. The T_g value used here is 206 K. Hoffman *et al.*[3] have suggested that U^* has a universal value of $6.28\,kJ\,mol^{-1}$ whereas Kovacs *et*

al.[6–10] quote a value of 29.3 kJ mol^{-1} and this is the value preferred by Cheng *et al.*[12], consequently we have used this latter value here.

Figure 9 clearly shows that two regimes are evident for PEO whereas for the blends only one growth regime prevails over the range of T_c investigated here. The ratio of the slopes of the two regions indicates that for $\Delta T \geq 21$ K regime II growth takes place and for $15\,\text{K} \leq \Delta T \leq 21\,\text{K}$ regime I growth is evident. Cheng *et al.*[12] report for pure PEO that regime II growth takes place for supercoolings between 10 and 17.5 K and above this higher value of ΔT regime III growth takes place. Regime I growth appears to be confined to a very narrow range of ΔT between 8.5 and 10 K. Our data do not conform to the behaviour observed by Cheng *et al.* The slopes obtained from our data are almost exactly in the theoretical ratio of 2 expected and it is because the region of higher slope is at higher abscissa values that we make the regime assignments given above. Some of this difference in regime temperatures may be due to the different procedures used to initiate crystallization. Cheng *et al.*[12] used the seeding procedure of Kovacs whereas we have used no such method. On the basis of the similarity of the slopes to the value for PEO, the growth rate behaviour of the blends (*Figure 10*) has been assigned to regime II. The values of K_g(I) and K_g(II) (where appropriate) obtained are reported in *Table 5*.

Three regimes of growth behaviour appear to be evident for the block copolymer and these are marked on *Figure 11*. We point out that one of these regions (that for the smallest values of ΔT) is only defined by two data points and therefore its assignment from the current data is only tentative. The values of $K_g(i)$ are given in *Table 5* and on the basis of these values we have assigned them to regimes I, II and III; again we emphasize here that the value of K_g(I) is extremely tentative since it is based on two data points only. The value is included here to indicate that regime I behaviour appears to persist to larger values of supercooling in the copolymer than in the blends or the pure PEO.

For calculation of $\sigma\sigma_e$ from these $K_g(i)$ values we have used a value of 4.62 Å for the stem width b; these values are also given in *Table 5*. Values of $\sigma\sigma_e$ for pure PEO and from the blends data are relatively constant at ~260–270 erg^2 cm^{-4}; adopting a value of 10 erg cm^{-2} for σ, the fold surface free energy, σ_e, is ~26 erg cm^{-2}. This value is in good agreement with those of Cheng *et al.*[12] and Kovacs *et al.*[6–10] and thus it appears that the presence of PMMA has no influence on the crystallization of the PEO apart from suppressing regime I growth behaviour to lower supercooling values. This suppression may be due to rejection of PMMA molecules from the region of the growth surface (substrate) and the vacancies created acting as nucleating heterogeneities, thus extending the range of regime II by the multiplicity of nucleation sites present. In passing we note that

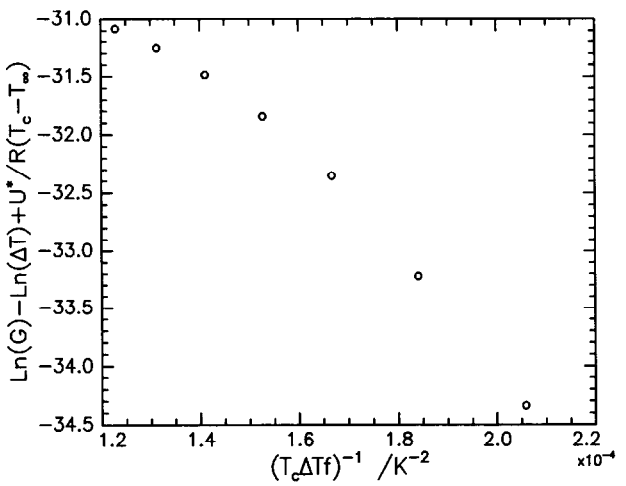

Figure 9 Plot of $\ln G + \ln \Delta T - U^*/(T_c - T_\infty)$ as a function of $(T_c \Delta T f)^{-1}$ for PEO

Table 5 Regime analysis slopes and surface free energy products

	Slope (K^{-2})			$\sigma\sigma_e$ (erg^2 cm^{-4})		
Polymer	I	II	III	I	II	III
PEO	−50 823	−25 554	–	272	270	–
BL90		−25 082	–	–	270	–
BL80	–	−24 156	–	–	259	–
BL70	–	−24 852	–	–	268	–
BC76	−28 890	−19 050	−36 962	200	206	160

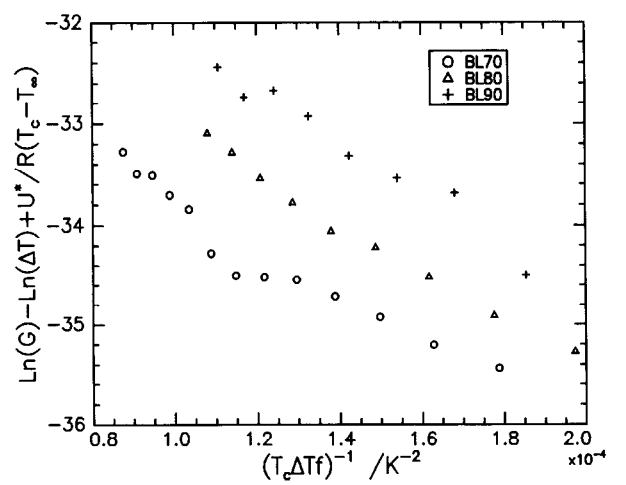

Figure 10 Plot of $\ln G + \ln \Delta T - U^*/(T_c - T_\infty)$ as a function of $(T_c \Delta T f)^{-1}$ for PMMA/PEO blends

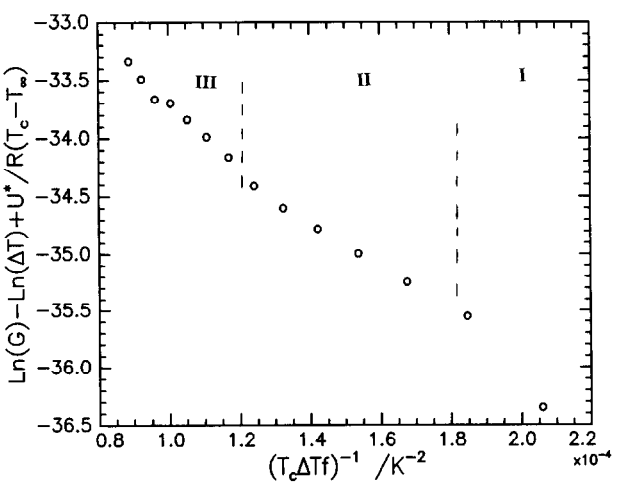

Figure 11 Plot of $\ln G + \ln \Delta T - U^*/(T_c - T_\infty)$ as a function of $(T_c \Delta T f)^{-1}$ for BC76

Calahorra *et al.*[28] have also found that σ_e is independent of PMMA content in PMMA/PEO blends and similarly Ong and Price[17] reported no dependence of σ_e on composition for poly(ϵ-caprolactone)/poly(vinyl chloride) mixtures.

This behaviour is to be contrasted with that of the block copolymer, BC76. The values of $\sigma\sigma_e$ calculated from the $K_g(i)$ values are reported in *Table 5*, and these are significantly reduced from those for the pure PEO or the blends. The fold surface free energy calculated for BC76 is in the region of 16–20 erg cm^{-2}. This decrease in σ_e is surprising in view of the fact that the fold surface is interfaced with the amorphous phase which contains PMMA. For PEO/PMMA blends, Martuscelli *et al.*[26] have proposed that the decrease in σ_e that they observed was due to increased entropy contributions due to entanglements between the PEO and PMMA, thus favouring loop formation at the fold surface. Although this may contribute to the reduction of σ_e a far greater contribution may be due to the very favourable enthalpy of mixing between PMMA and amorphous PEO. The fold surface is essentially liquid-like and thus will mix easily with the PMMA and hence the favourable mixing enthalpy will reduce the fold surface free energy. Why, then, does this not prevail in the blends? The PMMA is rejected from the growth front but in the block copolymer the PMMA cannot ever be distant from the crystalline regions because it is covalently bound to the PEO, consequently in the block copolymer the PMMA is always relatively close to the fold surface (indeed must emanate from it) and can thus interact easily with the PEO folds. In the blend, however, the PMMA has to diffuse from the growth front to the fold surface and this may be restricted by viscous resistance from surrounding PEO molecules attempting to crystallize on the growth front.

Differential scanning calorimetry: Avrami analysis

Since Avrami analysis to obtain macroscopic parameters of the crystallization kinetics requires a property dependent on the mass of crystalline material present, we have used the enthalpies of fusion obtained from the d.s.c. data of isothermal crystallization. Our aims here are to ascertain whether copolymerization has influenced the growth morphology or the macroscopic mechanism of nucleation and growth. For this analysis $X(t)$ is defined by:

$$1 - X(t) = (\Delta_{fus}H_{t=\infty} - \Delta_{fus}H_t) \div (\Delta_{fus}H_{t=\infty} - \Delta_{fus}H_{t=0}) \quad (6)$$

where $\Delta_{fus}H_{t=\infty}$ and $\Delta_{fus}H_t$ are the enthalpies of fusion on complete crystallization and after time t. The zero time was taken to be the instant when the temperature reached T_c. This results in the exponent n being dependent upon all three factors, type of nucleation, growth morphology and growth control, in the kinetics of crystallization.

Figure 12 shows the double logarithmic plot for the Avrami analysis of enthalpy of fusion data for BC76. From the initial slopes for each T_c a value for n has been obtained and log K_n evaluated from the intercept. *Tables 6* and *7* list the values of n and log (K_n) determined for BC76 and the PEO/PMMA blends, respectively.

No discernible difference between the block copolymer and the blends in the average value of n is apparent, since both types of system have $n = 3.8 \pm 0.2$. This value is close to the theoretical value of 4.0 predicted for homogeneous nucleation of spherical growth entities whose growth is controlled by the rate of attachment of molecules to the growth surface at the interface between

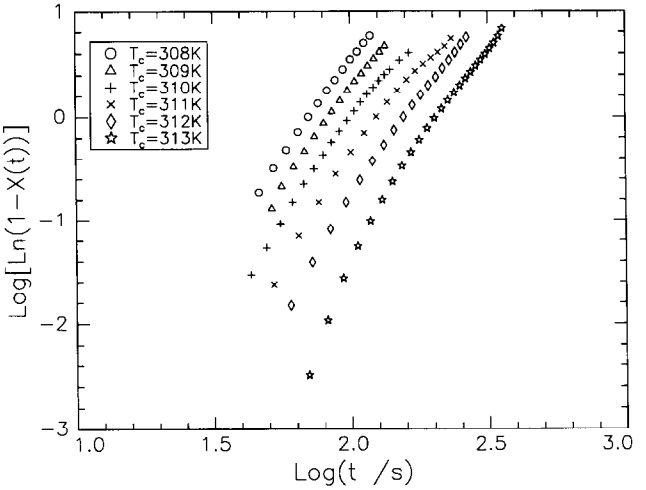

Figure 12 Avrami analysis of enthalpy of fusion data for BC76. Equation (6) defines $(1 - X(t))$

Table 6 Evaluated Avrami parameters for BC76 obtained by isothermal crystallization and differential scanning calorimetry

T_c (K)	Log K_n	n
316	−10.9	4.0
315	−9.63	3.9
314	−8.97	3.8
313	−8.94	3.9
312	−8.33	3.8
311	−7.96	3.8
310	−7.66	3.8
309	−7.19	3.7
308	−6.81	3.7

Table 7 Evaluated Avrami parameters for PEO and its blends with PMMA obtained by isothermal crystallization and differential scanning calorimetry

PEO						
T_c (K)	325	323	321	319	317	
Log K_n	−9.35	−8.84	−7.59	−7.12	−6.21	
n	3.6	4.0	3.9	4.0	3.8	
PMMA/PEO (90/10) BL90						
T_c (K)	323	321	319	317	315	
Log K_n	−9.73	−8.16	−7.81	−7.42	−6.97	
n	3.7	3.5	3.7	3.9	3.9	
PMMA/PEO (80/20) BL80						
T_c (K)	321	319	317	315	313	
Log K_n	−10.10	−9.30	−8.74	−7.99	−7.45	
n	3.9	3.9	3.9	3.8	3.8	
PMMA/PEO (70/30) BL70						
T_c (K)	317	315	313	311	309	307
Log K_n	−10.14	−8.66	−8.77	−8.25	−8.17	−7.5
n	4.0	3.6	3.9	3.9	4.1	3.9
PMMA/PEO (60/40) BL60						
T_c (K)	311		309	307		305
Log K_n	−9.39		−8.77	−6.66		−6.18
n	3.7		3.4	2.7		2.6

the melt and the crystalline region. The irregular values in n and K_n for BL60 are due to the phase separation process proposed to take place at larger values of supercooling. A very small decrease in the value of n as T_c decreases is apparent and a similar but more obvious trend in n for PEO/PMMA blends has been observed by Calahorra *et al.*[27]

Figure 13 shows the effective rate constant (K_n) obtained from the Avrami analysis plotted as a function of the supercooling for BC76 and PEO. For pure PEO all the data are confined to regime I growth whilst for BC76 the data points at $\Delta T \cong 14.8$ and 15.8 K may be in regime I (from comparison with OM data), the remainder appear to be in regime II. All of the data for the blends were in regime II. Consequently there is broad agreement in the regime behaviour in the d.s.c. with that observed by the more direct means of OM.

The values of n calculated here for PEO/PMMA blends are appreciably higher than those previously reported[26,27]. *Table 8* collects together the values of n and a clear trend is observable. The exponent increases as the overall molecular weight of the PEO/PMMA blend decreases. This may be attributable to the growth becoming diffusion-controlled at higher blend molecular weights due to the higher viscosities which prevail in the melt.

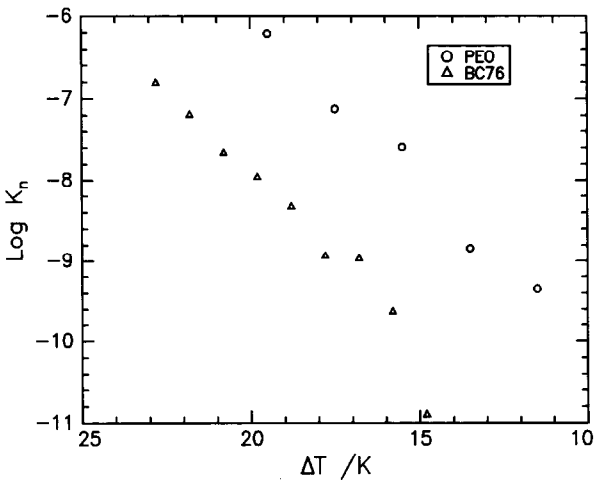

Figure 13 Log K_n values obtained from Avrami analysis of enthalpy of fusion data as a function of ΔT for BC76 and PEO

Table 8 Average JMA exponents for various molecular weights of PEO/PMMA blends

PEO/PMMA (w/w)	PEO (M_n 18.6 × 10^3)[a] PMMA (M_n 22.2 × 10^3)	PEO (M_w 100 × 10^3)[b] PMMA (M_w 110 × 10^3)	PEO (M_w 4000 × 10^3)[c] PMMA (M_w 93.6 × 10^3)
100/0	3.8 ± 0.2[d]	2.6	1.9
90/10		2.6	2.0
80/20		2.5	2.1
70/30		2.8	2.3
60/40		3.1	2.7

[a] Present work, from d.s.c. data
[b] Ref. 6, from d.s.c. data
[c] Ref. 7, from depolarization microscopy measurements
[d] Independent of composition

CONCLUSIONS

A 3–4-fold decrease in the rate of isothermal crystallization of PEO and a 2–3 K lowering of the equilibrium melting point are observed in a linear diblock copolymer of poly(ethylene oxide) and poly(methyl methacrylate), PEO-*b*-PMMA, containing 76% (w/w) of PEO, in comparison with the corresponding blend. The fold surface free energy of the crystalline regions in the block copolymer, obtained by crystalline regime analysis, is ~16–20 erg cm^{-2} and this is considerably lower than the value obtained for the pure poly(ethylene oxide) or the blends. This reduction in fold surface free energy has been attributed to a favourable enthalpy of mixing which is assisted by the proximity of the PMMA block to the fold surface. The presence of the PMMA in the blend appears to suppress regime I crystallization to lower temperatures. The block copolymer displays all three crystallization regimes, although the allocation of regime I from the current data is extremely tentative. Enthalpies of fusion obtained from isothermal crystallization in the d.s.c. have been used in an Avrami analysis to obtain the Avrami exponent and an effective rate constant. The block copolymer, the blends and pure poly(ethylene oxide) all display homogeneous nucleation with spherical growth geometry which is controlled by the rate of attachment to the growing surface. Comparison with Avrami exponents for blends of higher molecular weight suggests that the growth control mechanism changes to diffusion control which may be due to the higher viscosity of the melts.

ACKNOWLEDGEMENTS

P.H.R. thanks the Science and Engineering Research Council for the provision of a maintenance award throughout the course of the work, of which part is reported here. R.W.R. and P.H.R. thank ICI plc Wilton Materials Centre for partial financial support of this work via a CASE award and specific contributions which enabled apparatus construction.

REFERENCES

1 Johnson, W. A. and Mehl, R. F. *Trans. AIME* 1939, **A16**, 135
2 Avrami, M. *J. Chem. Phys.* 1939, **7**, 1103; 1940, **8**, 212; 1941, **9**, 177
3 Hoffman, J. D., Davis, G. T. and Lauritzen, J. I. Jr in 'Treatise on Solid State Chemistry' (Ed. N. B. Hanney), Plenum Press, New York, 1976, Vol. 3, Ch. 7
4 Hoffmann, J. D. and Miller, R. L. *Macromolecules* 1988, **21**, 3038
5 Hoffman, J. D. *Faraday Discuss. Chem. Soc.* 1979, **68**, 386
6 Kovacs, A. J. and Gonthier, A. *Kolloid Z.Z Polym.* 1972, **250**, 530
7 Kovacs, A. J., Gonthier, A. and Straupe, C. *J. Polym. Sci., Polym. Symp.* 1975, **50**, 283
8 Kovacs, A. J., Straupe, C. and Gonthier, A. *J. Polym. Sci., Polym. Symp.* 1977, **59**, 31
9 Kovacs, A. J. and Straupe, C. *Faraday Discuss. Chem. Soc.* 1979, **68**, 225
10 Kovacs, A. J. and Straupe, C. *J. Cryst. Growth* 1980, **48**, 210
11 Ding, N. and Amis, E. J. *Macromolecules* 1991, **24**, 3906
12 Cheng, S. Z. D., Chen, J. and Janimak, J. J. *Polymer* 1990, **31**, 1018
13 Cheng, S. Z. D., Zhang, A., Barley, J. S., Chen, J., Habenschuss, A. and Zschack, P. R. *Macromolecules* 1991, **24**, 3937
14 Cheng, S. Z. D., Chen, J., Zhang, A., Barley, J., Habenschuss, A. and Zschack, P. R. *Polymer* 1992, **33**, 1140

15 Martuscelli, E. *Polym. Eng. Sci.* 1984, **24**, 8
16 Wang, T. T. and Nishi, T. *Macromolecules* 1977, **10**, 421
17 Ong, C. J. and Price, F. P. *J. Polym. Sci., Polym. Symp.* 1978, **63**, 59
18 Cortazar, M. M., Calahorra, M. E. and Guzmán, G. M. *Eur. Polym. J.* 1982, **18**, 165
19 Li, X. and Hsu, S. L. *J. Polym. Sci. Polym. Phys. Edn* 1984, **22**, 1331
20 Sanchez, I. C. in 'Polymer Blends', (Eds D. R. Paul and S. Newman), Academic Press, New York, 1978, p. 135
21 Martuscelli, E., Demma, G., Rossi, E. and Segre, A. L. *Polymer* 1983, **24**, 266
22 Silvestre, C., Cimmino, S., Martuscelli, E., Karasz, A. L. and MacKnight, W. J. *Polymer* 1987, **28**, 7
23 Martuscelli, E., Silvestre, C., Addonizio, M. L. and Amelino, L. *Makromol. Chem.* 1986, **187**, 1557
24 Li, X. and Hsu, S. L. *J. Polym. Sci., Polym. Phys. Edn* 1984, **22**, 1331
25 Cimmino, S., Di Pace, E., Martuscelli, E. and Silvestre, C. *Makromol. Chem. Rapid Commun.* 1988, **9**, 261
26 Martuscelli, E., Pracella, M. and Yue, W. P. *Polymer* 1984, **25**, 1097
27 Calahorra, E., Cortazar, M. and Guzmán, G. M. *Polym. Commun.* 1983, **24**, 211
28 Calahorra, E., Cortazar, M. and Guzmán, G. M. *Polymer* 1982, **23**, 1327
29 Shultz, J. 'Polymer Materials Science', Prentice Hall, Englewood Cliffs, NJ, 1974, Ch. 9
30 Samuels, R. J. *J. Polym. Sci., A-2* 1971, **9**, 2165
31 Haudin, J. M. in 'Optical Properties of Polymers' (Ed. G. H. Meeten), Elsevier, London, 1986
32 Martuscelli, E. and Demma, G. in 'Polymer Blends: Processing, Morphology and Properties' (Eds E. Martuscelli, R. Palumbo and M. Kryszewski), Plenum, New York, 1980
33 Martuscelli, E., Canetti, M., Vicini, L. and Seves, A. *Polymer* 1982, **23**, 331
34 Okado, T., Saito, H. and Inoue, H. *Macromolecules* 1990, **23**, 3865
35 Cahn, J. W. in 'Crystal Growth' (Ed. H. S. Peiser), Pergamon, New York, 1967, p. 68
36 Hoffman, J. D. and Weeks, J. J. *J. Res. Natl. Bur. Stand., A* 1962, **66**, 13
37 Hopkinson, I. and Richards, R. W. unpublished results
38 Nishi, T. and Wang, T. T. *Macromolecules* 1975, **8**, 909
39 Hoffman, D. M. *PhD Thesis*, University of Massachusetts, 1979
40 Donth, E., Kretzschmar, H., Schulze, G., Garg, D., Höring, S. and Ulbricht, J. *Acta Polym.* 1987, **38**, 261